Bottom-up approach to the Galactic Center excess

Eder Izaguirre,[1] Gordan Krnjaic,[1] and Brian Shuve[1,2]

[1]*Perimeter Institute for Theoretical Physics, Waterloo, Ontario N2L 2Y5, Canada*
[2]*Department of Physics and Astronomy, McMaster University, Hamilton, Ontario L8S 4L8, Canada*

It has recently been shown that dark-matter annihilation to bottom quarks provides a good fit to the Galactic Center gamma-ray excess identified in the Fermi-LAT data. In the favored dark-matter mass range $m \sim 30$–40 GeV, achieving the best-fit annihilation rate $\sigma v \sim 5 \times 10^{-26}$ cm^3 s^{-1} with perturbative couplings requires a sub-TeV mediator particle that interacts with both dark matter and bottom quarks. In this paper, we consider the minimal viable scenarios in which a Standard Model singlet mediates s-channel interactions *only* between dark matter and bottom quarks, focusing on axial-vector, vector, and pseudoscalar couplings. Using simulations that include on-shell mediator production, we show that existing sbottom searches currently offer the strongest sensitivity over a large region of the favored parameter space explaining the gamma-ray excess, particularly for axial-vector interactions. The 13 TeV LHC will be even more sensitive; however, it may not be sufficient to fully cover the favored parameter space, and the pseudoscalar scenario will remain unconstrained by these searches. We also find that direct-detection constraints, induced through loops of bottom quarks, complement collider bounds to disfavor the vector-current interaction when the mediator is heavier than twice the dark-matter mass. We also present some simple models that generate pseudoscalar-mediated annihilation predominantly to bottom quarks.

I. INTRODUCTION

Although dark matter (DM) constitutes roughly 85% of the matter in our Universe, its identity and interactions are currently unknown [1]. If DM annihilates to visible states, existing space-based telescopes may be sensitive to the flux of annihilation byproducts arising from regions of high DM density, including the Galactic Center (GC).

Several groups have confirmed a statistically significant excess in the Fermi-LAT gamma-ray spectrum [2–11], originally identified in [12]. The excess is largely confined to an angular size of $\lesssim 10°$ with respect to the GC, exhibits spherical symmetry, and is uncorrelated with the Galactic disk or Fermi bubbles [9]. While this excess may still be astrophysical in origin, potentially due to an unusual population of millisecond pulsars [7], its energy spectrum and spatial distribution are well modeled by a Navarro-Frenk-White profile [13] of dark-matter particles $\chi\bar{\chi}$ annihilating to $b\bar{b}$ with mass and cross section [8]

$$\langle \sigma v \rangle = (5.1 \pm 2.4) \times 10^{-26} \text{ cm}^3 \text{ s}^{-1}, \tag{1}$$

$$m_\chi = 39.4(^{+3.7}_{-2.9} \text{ stat.})(\pm 7.9 \text{ sys.}) \text{ GeV}, \tag{2}$$

which are compatible with a DM abundance from thermal freeze-out.

Recent work has presented the collider and direct-detection constraints on this interpretation assuming flavor-universal and mass-proportional couplings to SM fermions [14,15]; these analyses apply collider bounds on DM production assuming a contact interaction between dark and visible matter. The analyses in [15–17] also study simplified models of DM annihilation mediated by color-charged t-channel mediators. For perturbative interactions, Eq. (2) implies that the mediator mass is below a TeV, so it can be produced on shell at the Large Hadron Collider (LHC) and decay to distinctive final states with a mixture of b jets and missing energy (E_T). At direct-detection experiments, this mediator can also be integrated out to induce dark-matter scattering through loops of b quarks that exchange photons or gluons with nuclei. Up to differences in Lorentz structure, these processes are generic predictions of any model that explains the Fermi anomaly; however, for light mediators ($< 2m_\chi$), it is possible to evade collider searches [18].

In this paper, we study the scenario with an s-channel mediator that predominantly couples to b quarks and focus on the regime in which the mediator is $\gtrsim 100$ GeV and can decay to pairs of DM particles. The mediator can be produced in processes involving b quarks, and its decays yield final states with b jets and/or missing energy. We extract constraints from LHC searches for new physics in the $b\bar{b} + E_T$ final state and explore the sensitivity of a proposed mono-$b + E_T$ analysis [19]. We find that large regions of favored parameter space are excluded by existing 8 TeV sbottom searches, whose sensitivity is projected to improve at 13 TeV. The mono-b analysis is expected to be comparable at 8 TeV and set stronger constraints at 13 TeV. We also clarify the LUX limits [20] on scattering through loops of b quarks and find strong bounds on the parameter space of vector mediators that explain the Fermi excess.

The organization of the paper is as follows: In Sec. II, we discuss a set of possible minimal interactions that can explain the GC excess. In Sec. III, we consider direct-detection, resonance, and Higgs search constraints on these scenarios. In Sec. IV, we show the constraints on these DM interpretations from sbottom LHC searches, which allow for a possible independent, complementary confirmation of the GC excess. We also estimate the reach of a mono-b search at 8, and extend our results for both searches to 13 TeV. In Sec. V, we outline concrete models that generate a pseudoscalar-mediated annihilation, which is the least constrained of all possible operators that can explain the gamma-ray anomaly.

II. ANNIHILATION OPERATORS

In the simplest models, dark matter can consist of fermions, scalars, or vector bosons. To narrow the scope of our investigation without essential loss of generality, we consider only parity-conserving interactions between dark and visible matter. For scalar DM, the leading-order interaction with $b\bar{b}$ is either ruled out by direct-detection bounds or the annihilation is p-wave suppressed [15], so achieving the rate in Eq. (1) in the latter case requires nonperturbative couplings. For vectors, protecting the DM from prompt decays requires nontrivial model building, so for simplicity we omit this possibility. Thus, for the remainder of this paper we focus exclusively on Dirac fermion DM candidates; Majorana particles are qualitatively similar, and the collider bounds are expected to be comparable.

We separately consider the following interactions:

$$\mathcal{L}_U = (g_\chi \bar{\chi}\gamma^\mu\gamma^5\chi + g_b \bar{b}\gamma^\mu\gamma^5 b)U_\mu, \tag{3}$$

$$\mathcal{L}_V = (g_\chi \bar{\chi}\gamma^\mu\chi + g_b \bar{b}\gamma^\mu b)V_\mu, \tag{4}$$

$$\mathcal{L}_a = i(g_\chi \bar{\chi}\gamma^5\chi + g_b \bar{b}\gamma^5 b)a, \tag{5}$$

where U, V, and a are axial-vector, vector, and pseudo-scalar fields that mediate s-channel χ and b interactions. We assume the mediator is a singlet under SM gauge interactions, and thus we do not address t-channel mediators in this article (see Ref. [15] for constraints on the latter). Our collider and direct-detection constraints assume only these interactions between the SM and DM. To leading order in velocity, the annihilation cross sections are

$$\langle\sigma v\rangle_U \simeq \frac{N_c}{2\pi}\frac{(g_\chi g_b)^2 m_b^2(1 - 4m_\chi^2/m_U^2)^2\sqrt{1 - m_b^2/m_\chi^2}}{(m_U^2 - 4m_\chi^2)^2 + m_U^2\Gamma_U^2}, \tag{6}$$

$$\langle\sigma v\rangle_V \simeq \frac{N_c}{\pi}\frac{(g_\chi g_b)^2 m_\chi^2(1 + m_b^2/2m_\chi^2)\sqrt{1 - m_b^2/m_\chi^2}}{(m_V^2 - 4m_\chi^2)^2 + m_V^2\Gamma_V^2}, \tag{7}$$

$$\langle\sigma v\rangle_a \simeq \frac{N_c}{2\pi}\frac{(g_\chi g_b)^2 m_\chi^2\sqrt{1 - m_b^2/m_\chi^2}}{(m_a^2 - 4m_\chi^2)^2 + m_a^2\Gamma_a^2}, \tag{8}$$

where $N_c = 3$ is the number of colors. For $g_b g_\chi = 1$, the best-fit values from Eq. (1) imply mediator masses in the few-hundred GeV range, which are light enough to be accessible with a combination of experimental strategies. For lighter mediators, the constraints due to direct-detection and collider experiments are quite weak and consistent with a DM interpretation of the gamma-ray excess [18]. In Secs. III and IV, we discuss the various constraints on the three sets of interactions [Eqs. (3), (4), (5)] from direct-detection experiments and collider searches.

III. DIRECT DETECTION AND RESONANCE SEARCHES

A. Direct detection

We consider first the vector interaction, which induces a spin-independent coupling between dark matter and nucleons. The LUX experiment currently places the strongest limit on spin-independent χ-nucleon interactions over the $m_\chi \sim 10$–100 GeV range, at $\sigma_{\rm SI} \lesssim 10^{-46}$ cm^2 [20]. Although we assume that V does not couple directly to light quarks, it is still possible for DM to induce elastic nuclear scattering through a loop of b quarks; the leading diagram is depicted in Fig. 1 and is mediated by a photon. The corresponding single-gluon diagram vanishes due to the color structure of the diagram. Ignoring electroweak effects, higher-order gluon processes are also zero, which is understood most simply by noting that vector-current conservation fixes the mapping of b-quark matrix elements into nucleon matrix elements to all orders in the strong interactions; the resulting amplitude is proportional to the net number of b quarks in the nucleon [21]. Since the numbers of b and $\bar{b}$ quarks in the nucleon are the same, the resulting direct-detection rate is zero up to electroweak corrections.

The cross section for the photon-induced vector-mediated process in the leading-log approximation is [22]

$$\frac{d\sigma}{dE} = \frac{(g_b g_\chi)^2 m_{\rm T}}{18\pi v^2 m_V^4}\left(\frac{\alpha Z}{\pi}\right)^2 F^2(E)\left[\log\left(\frac{m_b^2}{m_V^2}\right)\right]^2, \tag{9}$$
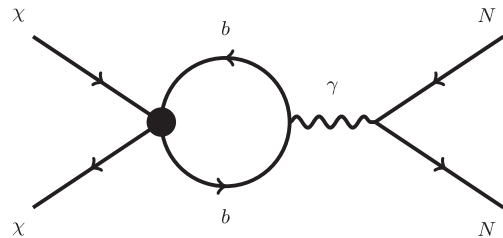

FIG. 1. Minimal loop-induced nucleon scattering at direct-detection experiments for an s-channel mediator particle between χ and b. The mediator has been integrated out.

where E is the nuclear recoil energy, m_T is the mass of a target nucleus, Z is the target's electric charge, v is the relative velocity, and F is the Helm form factor [23]. The scattering rate in units of counts/day/keV/kg detector mass is

$$\frac{dR}{dE} = \frac{\rho_\chi}{m_\chi m_T} \int_{v_{\min}(E)}^{v_{\rm esc}} d^3 v f_\odot(\vec{v}, v_0) v \frac{d\sigma}{dE}, \qquad (10)$$

where $\rho_\chi = 0.3~{\rm GeV/cm}^3$ is the local DM mass density, $v_{\min}(E) = \sqrt{m_T E / 2\mu}$ is the minimum DM velocity required to induce a nuclear recoil of energy E, $\mu = m_\chi m_T / (m_\chi + m_T)$ is the reduced mass, $v_{\rm esc} \approx 550~{\rm km/s}$ is the halo escape velocity, and $v_0 = 220~{\rm km/s}$ is the mean local DM velocity. Here, $f_\odot(\vec{v}, v_0)$ is the local DM velocity distribution in the detector frame, which is obtained from a Maxwellian distribution in the Galactic rest frame boosted by the Earth's velocity with respect to the halo.

Using the LUX limits and detection efficiencies [20], we find that the $(\bar{\chi}\gamma^\mu\chi)(\bar{b}\gamma_\mu b)$ interaction is disfavored over much of the $m_V > 2m_\chi$ range as shown in Fig. 3.[1]

For the pseudoscalar and axial-vector interactions in Eqs. (3) and (5), the diagram in Fig. 1 and higher-loop processes vanish due to the antisymmetric nature of the gamma-matrix trace in the loop [22], and thus direct-detection experiments do not constrain these scenarios.

B. Resonance searches

We consider constraints on nonstandard b-jet production in the context of dijet resonances and non-SM Higgs searches. Mediator production at hadron colliders proceeds via

$$pp \to U/V/a \to b\bar{b} \qquad (11)$$

and yields dijet resonances. The best limits are from UA2 and Tevatron dijet searches [25], which bound a universal Z' coupling by $\lesssim < 0.5$ over the $m_{Z'} \in 100$–1000 GeV range. In our scenarios of interest, the mediators couple only to b quarks, so the production rate is suppressed by parton distribution functions and there is no constraint for perturbative mediator couplings to b.

Similarly, the CMS search for nonstandard Higgs sectors is sensitive to final states with three or more jets [26], which can arise in our scenarios of interest via

---

[1] Our LUX limit on the $(\bar{\chi}\gamma^\mu\chi)(\bar{b}\gamma_\mu b)$ interaction (green curve in Fig. 3) disagrees with the bounds on spin-1 s-channel interactions in Fig. 3 of [15], which cites [24] for the loop-induced scattering cross section. However, the diagrams calculated in Appendix A of [24] feature a t-channel χb interaction, whereas the vector-vector interaction with an s-channel mediator arises from the process depicted in Fig. 1, which sets a stronger bound on this process.

$$pp \to (U/V/a \to b\bar{b}) + b{\rm jets}. \qquad (12)$$

Simulating inclusive U, V, and a production using MADGRAPH 5 [27], and applying the CMS limits from [26], we find this bound to be comparable to the sbottom and mono-b searches considered in Sec. IV for pseudo-scalars when $g_b = g_\chi$ (see Fig. 5). A similar bound is expected for axial-vector and vector mediators; however, the different kinematics of the (axial-)vector final states prevent a direct application of the bound, and the Higgs searches are subdominant to the sbottom constraints for these mediators anyway. In the $|g_\chi| \gg |g_b|$ limit, the multi-b Higgs search no longer applies, as the coupling to b quarks is relatively suppressed.

IV. COLLIDER DM SEARCHES

Collider studies of DM production in association with SM particles have proliferated vastly in recent years [17,28–52]. In this section, we consider interactions in which DM couples predominantly to b quarks through the axial-vector, vector, and pseudoscalar interactions [Eqs. (3)–(5)]. Although DM annihilation in the GC is well approximated by the contact-interaction limit for $m_\chi \ll m_{a,V,U}$, the preferred mediator masses are of order a few hundred GeV for perturbative couplings. Therefore, due to the high partonic center-of-mass energies at the LHC, the effective theory description [15,49,53] is not applicable. In this section, we show the LHC's sensitivity to on-shell production of pseudoscalar, vector, and axial-vector mediators, highlighting the parameter space suggested by the Fermi excess. The generic DM production process at the LHC is

$$pp \to (U/V/a \to \chi\bar{\chi}) + X_{\rm sm}, \qquad (13)$$

where $X_{\rm sm}$ can be any multiplicity of SM final states and the $U/V/a \to \chi\bar{\chi}$ decay yields missing energy in the final state. There are several scenarios to consider, depending on the nature of the additional SM final states, $X_{\rm sm}$, produced in association with $U/V/a$. For $X_{\rm sm} = W^\pm$, $X_{\rm sm} = Z^0$, or $X_{\rm sm} = j(\neq b)$, the signal could appear in the mono-$X_{\rm sm} + E_T$ searches [14].

However, the best sensitivity to these signals utilizes the power of b tagging, since mediator production is almost always accompanied by at least one associated b quark. Figure 2 depicts representative Feynman diagrams that give rise to b quarks and missing energy from DM production processes. Reference [19] proposed a mono-b analysis which can set strong constraints on the topologies considered in this article by looking for a b-tagged jet and significant missing energy. To date, this analysis has not yet been performed.

A central result of our paper is that strong bounds can already be set with existing LHC sbottom searches in the $2b + E_T$ channel. We note that this final state was
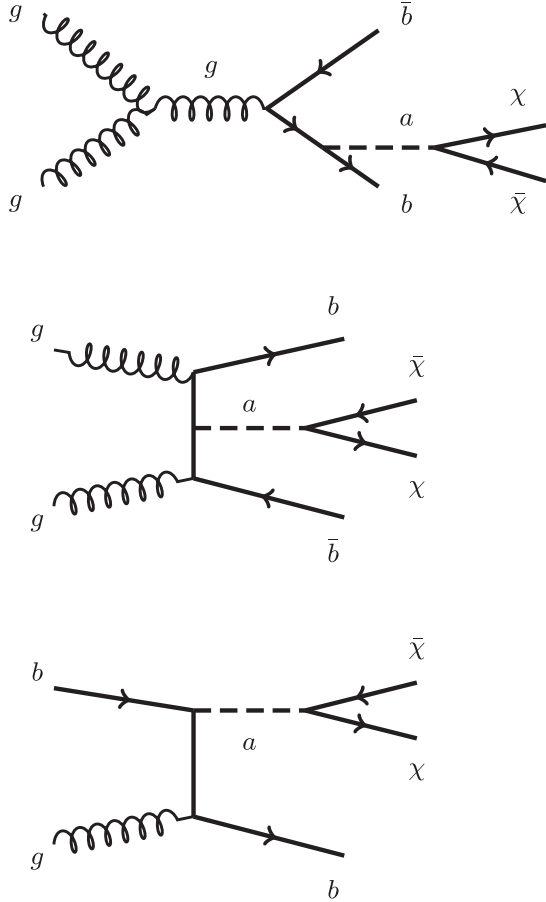
FIG. 2. Example diagrams for $pp \to b\bar{b}\chi\bar{\chi}$. If kinematically allowed, the dominant process is $pp \to b\bar{b}(a \to \chi\bar{\chi})$, which suffers less phase space suppression.
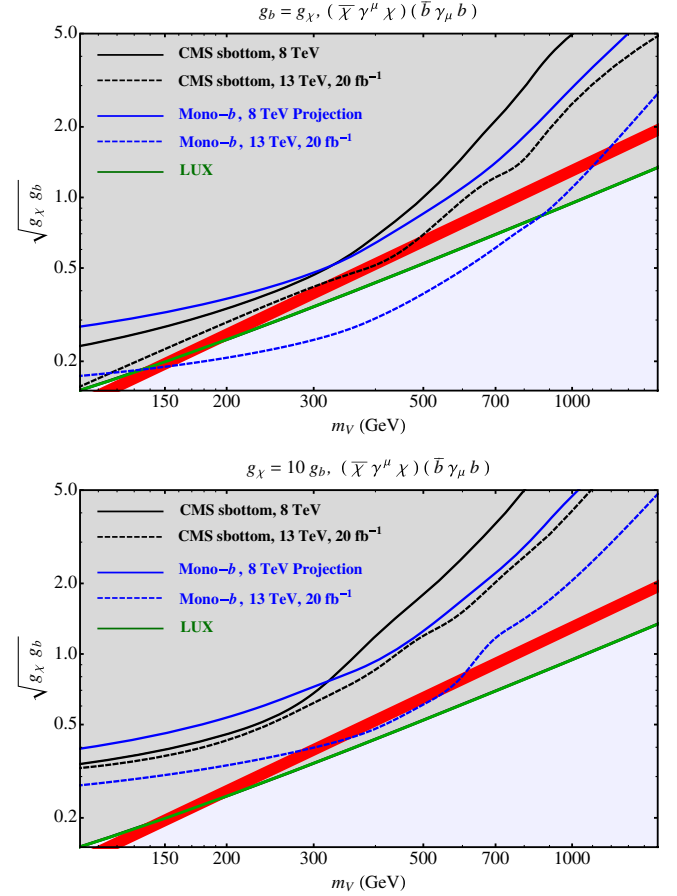

FIG. 3 (color online). Direct-detection and collider constraints on the vector-mediated scenario. The red band is the favored region for the $\chi\bar{\chi} \to V^* \to b\bar{b}$ annihilation in the GC [8]. The gray excluded region is extracted from the 8 TeV CMS sbottom search [62]—comparable limits arise from the ATLAS sbottom search in [61]—and the dashed blue line shows the projected sensitivity of the mono-b search using the cuts proposed in [19] at $\sqrt{s} = 8$ TeV. The green curve is the LUX bound using limits and efficiencies from [20].

considered by [15] in the context of the pair production of a colored t-channel mediator between b quarks and DM. Here, we show that the sbottom searches also place constraints on s-$channel$ mediators that are uncharged under the SM and are produced only through the interaction responsible for $\chi\bar{\chi} \to U/V/a \to b\bar{b}$ annihilation.

Our Monte Carlo calculations of the SM backgrounds for the mono-$b + \not{E}_T$ and $2b + \not{E}_T$ final states were done in MADGRAPH 5 [27]. We include samples of the dominant SM processes, namely, $V +$ jets and $t\bar{t} +$ jets, which are matched with the $k_\perp$-shower scheme [54]. Next-to-leading-order (NLO) k factors for the backgrounds are calculated with MCFM [55,56]. The pseudoscalar and axial-vector operators are also simulated in MADGRAPH 5 with a user-defined model. Showering and additional jets from initial- and final-state radiation are generated in PYTHIA 6.4 [57], with a detector simulation done in PGS 4 [58]. The PGS version used in this study is modified from the standard version [59]; in this modified PGS, the truth b and c tagging was improved, and the anti-k_T clustering was incorporated from [60]. This study uses an $R = 0.4$ clustering radius. We validated the backgrounds simulated in this study by

reproducing the expected background yield in the signal regions of the ATLAS sbottom search [61] to within 20%–30%.

Our main results are encapsulated in Figs. 3, 4, and 5, which present the constraints on the vector, axial-vector, and pseudoscalar operators, respectively. All three figures show constraints from collider production and direct detection for $g_\chi = g_b$ and $g_\chi = 10g_b$; the gray region in each plot is ruled out by existing searches, while the other curves show projections of potential future sensitivities. For clarity of presentation, we emphasize the CMS sbottom search [62], which already constrains a large region of parameter space for several scenarios, though comparable sensitivity is achieved with the corresponding ATLAS analysis [61]. The LHC is expected to have already put strong constraints on vector and axial-vector interactions for a range of parameter space that can explain the Fermi
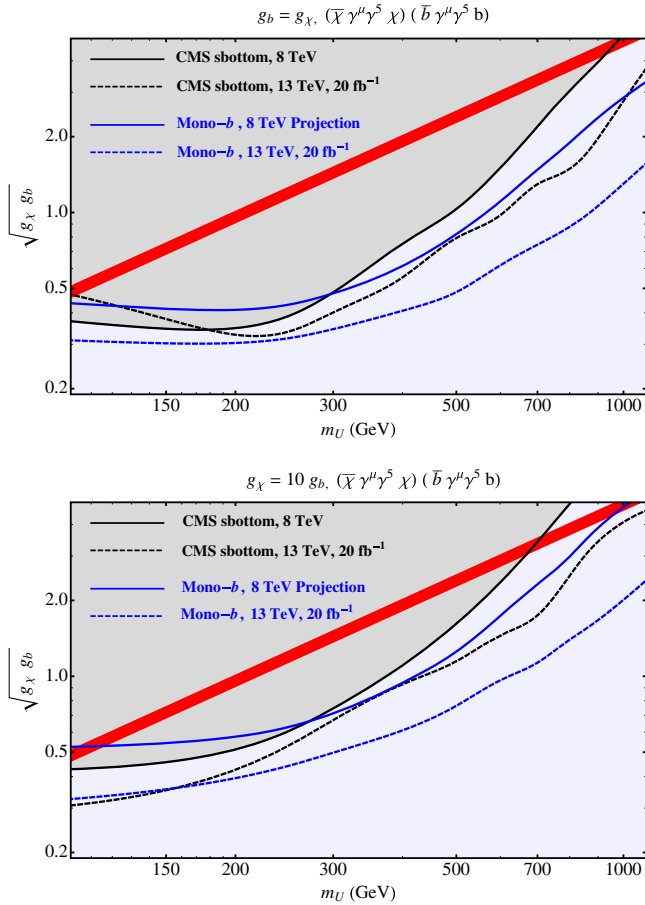
$g_b = g_\chi, \; (\overline{\chi}\,\gamma^\mu\gamma^5\,\chi)\,(\overline{b}\,\gamma^\mu\gamma^5\,b)$

$g_b = g_\chi, \; (\overline{\chi}\,\gamma^5\,\chi)\,(\overline{b}\,\gamma^5\,b)$

$g_\chi = 10\,g_b, \; (\overline{\chi}\,\gamma^\mu\gamma^5\,\chi)\,(\overline{b}\,\gamma^\mu\gamma^5\,b)$

$g_\chi = 10\,g_b, \; (\overline{\chi}\,\gamma^5\,\chi)\,(\overline{b}\,\gamma^5\,b)$

FIG. 4 (color online). Parameter space for the axial-vector-mediated scenario with constraints from the same searches and simulation details described in Fig. 3. For this interaction, DM-nucleus scattering induced by a *b*-quark loop is spin dependent, and there are no bounds on the favored parameter space from direct-detection experiments.
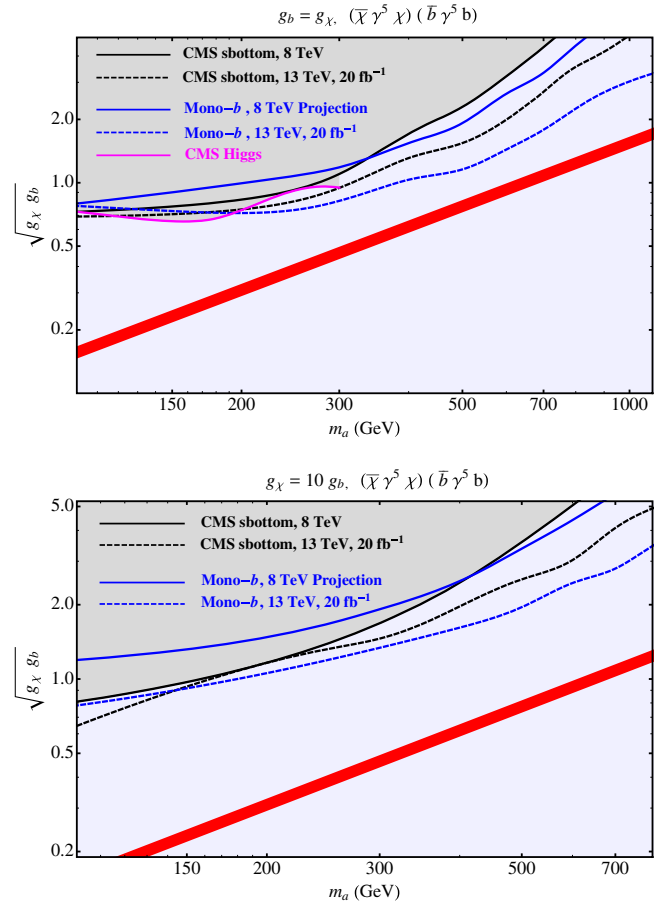
FIG. 5 (color online). Parameter space for the pseudoscalar-mediated scenario with constraints from the same searches and simulation details described in Fig. 3. For this interaction, DM-nucleus scattering induced by a *b*-quark loop is spin dependent and velocity suppressed, and there are no bounds on the favored parameter space from direct-detection experiments. Here we also include a constraint from the CMS Higgs search from [26].

gamma-ray excess. In the pseudoscalar scenario, however, the LHC constraints on the UV completion of this operator are not expected to robustly test the parameter spaced preferred by the gamma-ray excess.

The reasons for the weaker pseudoscalar limits are twofold. First, vectors and axial vectors have a larger number of degrees of freedom than pseudoscalars, resulting in a smaller production cross section for pseudoscalars due to the spin sums. The second effect is a mild difference in the pT distribution of a pseudoscalar vs a vector. Comparing associated pseudoscalar-*b* production with associated vector-*b* production, the pseudoscalar differential cross section is peaked towards smaller final-state momenta than the vector.[2] Therefore, when a cut is applied on the *b* jet(s) p_T and the E_T from the mediator decay into DM, the efficiency for passing that

cut is an $\mathcal{O}(1)$ factor smaller for the pseudoscalar scenario. Together, these factors contribute to a sufficiently weaker bound, such that the best-fit region for pseudoscalars is unconstrained.

In Figs. 3, 4 and 5, we also show our estimated sensitivity for 95% confidence level (CL) exclusion from future sbottom searches at 13 TeV, assuming the same selection criteria from the analysis at 8 TeV, with the addition of an optimization over missing transverse energy, E_T. The expected bounds that we draw at 13 TeV assume a systematic uncertainty of 10%. At 20 fb^{-1}, the signal regions we consider are already systematics dominated, and longer running will not necessarily improve the bounds.

We also show the sensitivity for 95% CL exclusion from a mono-*b* + E_T analysis proposed in [19] using the *b*-tagging working point from the CMS sbottom search [62]. This analysis offers more optimal coverage at high mediator masses, where the signal benefits from a hard radiated

---

[2]We have confirmed this analytically at matrix-element level for mono-*b* production, as well as in Monte Carlo simulation.

jet whose recoil boosts the $\chi\bar{\chi}$ system and consequently enhances the missing energy spectrum [63].

In Figs. 3, 4 and 5, we show how the bounds compare for $g_\chi = g_b$ and $g_\chi = 10g_b$. As we show in Sec. V, the g_b coupling is typically smaller than the g_χ coupling. For $g_\chi \gg g_b$, the bounds from LHC searches are weakened, as the rate for radiating off an on-shell mediator gets smaller.

In summary, we find that LHC searches with b jets and missing energy are excellent probes of interactions responsible for the GC excess, particularly for interactions mediated by axial vectors and vectors. In such scenarios, most of the parameter space with $m_{U,V} > 2m_\chi$ is already excluded or will be in early 13 TeV running. However, pseudoscalars currently evade all such constraints and will be challenging to probe at 13 TeV with heavy flavor + DM searches.

V. BEYOND THE MINIMAL INTERACTION

A. Pseudoscalar-mediated models

In this section, we study concrete models that give rise to $\bar{\chi}\chi \to \bar{b}b$ annihilation with pseudoscalar mediators. Our emphasis is motivated both by the larger allowed parameter space that remains for this scenario and the difficulty of constructing viable vector and axial-vector interactions that give rise to appreciable annihilation rates. Note that the interactions in Eq. (5) are not permitted prior to electroweak symmetry breaking as the left- and right-handed bottom quarks have different gauge charges. Therefore, we generically find that $g_\chi \gg g_b$ for a singlet mediator, as the coupling to the visible sector is often accompanied by some source of suppression (mixing angles, higher-dimensional operators, etc.).

1. Two-Higgs doublet model with a singlet

A pseudoscalar with the interactions in Eq. (5) can arise in a two-Higgs doublet model (2HDM) with an additional complex-scalar singlet. Two-Higgs doublet models typically induce flavor-changing neutral currents (FCNCs) that are strongly constrained unless each set of fermions couples predominantly to only one of the Higgs doublets [64]. We consider a scenario analogous to [65], where one of the Higgs doublets, which we refer to as H_u, couples to the up-type quarks and the leptons, while the other doublet, which we refer to as H_d, couples to the down-type quarks. The Lagrangian for this scenario contains

$$\mathcal{L} \supset g_\chi \mathcal{S}\bar{\chi}\chi + \lambda_d^{ij}\bar{Q}^i H_d d_R^j - \mu\mathcal{S}H_u H_d + \text{H.c.}, \quad (14)$$

where χ is a Dirac fermion uncharged under the SM, $\mathcal{S} = (\phi + ia)/\sqrt{2}$ is a complex scalar, and $H_{u,d} = (h_{u,d} + ia_{u,d})/\sqrt{2}$. In the $\tan\beta \equiv v_u/v_d \gg 1$ limit, $v_u \approx v = 246$ GeV, the down-type Yukawa coupling λ_d is of order one, and $\mathcal{S}$ mixes predominantly with the down-type Higgs.

Assuming CP conservation, the scalars and pseudoscalars mix separately and acquire identical off-diagonal mass

terms $\sim \mu v/\sqrt{2}$. This mixing induces both the desired $\chi\bar{\chi} \to a \to b\bar{b}$ annihilation and scalar-mediated spin-independent scattering at direct-detection experiments, which is strongly constrained. Both processes are proportional to the mixing angles, which scale approximately as

$$\sin\theta_a \sim \frac{\mu v}{\sqrt{2}\mu v + m_a^2 + m_{a_d}^2}, \quad (15)$$

$$\sin\theta_\phi \sim \frac{\mu v}{\sqrt{2}\mu v + m_\phi^2 + m_{h_d}^2}, \quad (16)$$

in the limit where one mass term dominates both the numerator and denominator. m_{a,ϕ,a_d,h_d} are the tree-level mass terms prior to electroweak symmetry breaking.

In the absence of tuning, the lightest scalar and pseudoscalar have comparable tree-level masses and there is generic tension between ensuring a $\lesssim$TeV pseudoscalar with a large mixing angle to explain the Fermi excess and keeping at least one scalar component above $\gtrsim$TeV to suppress elastic spin-independent scattering at LUX [20]. To alleviate this tension, we can make the mixing angles hierarchical by ensuring $m_a \sim m_{a_d}$ and $m_\phi \gg m_{\phi_d}$, which implies a tuning in the $\mathcal{S}$ masses. The most general CP-conserving mass terms are

$$-\mathcal{L}_m \supset \mu_1^2|\mathcal{S}|^2 + \mu_2^2\text{Re}(\mathcal{S}^2), \quad (17)$$

which yield tree-level scalar and pseudoscalar mass terms

$$m_a^2 = \mu_1^2 - \mu_2^2, \quad (18)$$

$$m_\phi^2 = \mu_1^2 + \mu_2^2. \quad (19)$$

These masses can be split, given a degeneracy of μ_1 and μ_2. To quantify the necessary hierarchy, let $m_a = xm_\phi$, where

$$x \equiv \sqrt{\frac{(\mu_1 - \mu_2)(\mu_1 + \mu_2)}{(\mu_1^2 + \mu_2^2)}}. \quad (20)$$

Thus, the splitting has to be tuned by a factor x^2. For large pseudoscalar mixings, $\mu v \sim m_a \sim$ few hundred GeV, the mass ratio $m_a/m_\phi \gtrsim 10$ is required to evade LUX bounds on ϕ-mediated scattering. This corresponds to a tuning of order $x^2 \sim 1\%$.

2. Vectorlike quarks

It is also possible to induce the pseudoscalar couplings in Eq. (5) without extending the Higgs sector. Consider the SM with an additional singlet pseudoscalar, a, and three generations of vectorlike quarks, Ψ_i, with charge $(3,2)_{\frac{1}{6}}$ under $SU(3)_c \times SU(2)_L \times U(1)_Y$. Up to field redefinitions, the most general renormalizable interactions are

$$\mathcal{L} \supset y_{1ki}a\bar{\Psi}_k\gamma^5 Q_i + y_{2kj}\bar{\Psi}_k H d_R^j + M_{\Psi,k}\bar{\Psi}_k\Psi_k, \quad (21)$$

where H is the SM Higgs doublet. Integrating out Ψ yields the effective interaction

$$\mathcal{L}_{\text{eff}} = \frac{y_{ij}}{M_\Psi} \bar{Q}^i \gamma^5 d_R^j H a \to \frac{y_{ij} v}{\sqrt{2} M_\Psi} \bar{Q}^i \gamma^5 d_R^j a, \qquad (22)$$

where we define $y_{ij} \equiv \sum_k y_{1ki} y_{2kj}^*$. The effective Yukawa coupling must be aligned with the down-type Yukawa matrix to avoid FCNCs.

Since $v/\sqrt{2} \approx 174$ GeV, and with vectorlike quarks with SM-sized couplings constrained by the LHC to masses $\gtrsim 700$ GeV [66,67], requiring $y_{ij} \lesssim 2$ implies an upper bound of the effective $y_b \lesssim 0.5$.

B. Vector and axial-vector mediators

The simple models with vector or axial-vector mediators between dark matter and the SM are already under considerable tension from collider searches and, in the case of a vector mediator, direct-detection bounds. These constraints involve only the minimal interaction; however, more complete models will typically feature couplings between the (axial-)vector mediator and other SM fields. For instance, vector and axial-vector currents couple to both left- and right-handed fermions, and since left-handed bottom quarks are included in a weak doublet with left-handed top quarks, a coupling to tops is generically expected as well. We consider vector and axial-vector interactions that couple preferentially to third-generation quarks; such couplings must align with the mass eigenstates to avoid FCNCs, and there must be additional spectator fields to cancel anomalies. We defer a discussion of such extra model components, however, and instead focus on how the constraints in Sec. IV change if the (axial-)vector mediator additionally couples to tops, since this is the most model-independent extension of the coupling to b quarks in Eqs. (3) and (4).

For $m_{U,V} \gtrsim 350$ GeV, the collider constraints from sbottom and mono-b searches are modified; the decay mode $U, V \to t\bar{t}$ suppresses the DM production rate. For $g_b = g_\chi$, this weakens all bounds on $\sqrt{g_\chi g_b}$ by approximately $\sqrt{2}$. This does not qualitatively change our conclusions, although some regions of parameter space may not be excluded until the 13 TeV running. For $g_\chi = 10 g_b$, however, there is no change in the bound because the mediator nearly always decays into $\chi\bar{\chi}$.

New production and decay modes of the mediator are now possible with $g_b = g_t$. The same mediator production processes considered in Sec. IV, namely, $pp \to b + U/V$, $b\bar{b} + U/V$, now lead to $t\bar{t}b\bar{b}$ production from $U/V \to t\bar{t}$. This modifies the total top-quark production cross section. Because of the larger coupling for axial-vector scenarios, requiring a contribution to the total $t\bar{t}$ cross section [68] of $< 10\%$ excludes axial-vector masses in the range $m_U \approx$ 350–500 GeV for the Fermi-favored region, while there is no bound for vector mediators from $\sigma_{t\bar{t}}$.

Similarly, the mediator can now be produced via the top coupling. Production proceeds through $pp \to t\bar{t} + Z'$, as well as by gluon fusion through a top loop. For equal couplings to top and bottom, the production rate through the b coupling is much larger since there is no mass or loop suppression of the rate. Still, we confirmed that SM $t\bar{t}$ + Higgs searches do not constrain the Fermi-favored region. We have also considered potential bounds from stop searches [69] and found these to be less sensitive than sbottom searches due to the smaller production cross section.

VI. CONCLUSION

In this paper, we have studied the direct-detection and collider constraints on SM singlet particles that mediate s-channel interactions between DM and b quarks, assuming the mediator can decay to DM particles. For simplicity, we have emphasized only parity-conserving interactions between dark and visible sectors, which restricts the class of operators whose annihilation rate is unsuppressed by powers of relative velocity. This is the minimal extension to the SM that suffices to explain the Galactic Center gamma-ray excess identified in the Fermi-LAT data. Our main results are as follows:

(i) Direct-detection results from LUX disfavor a vector-vector interaction $(\bar{\chi}\gamma^\mu\chi)(\bar{b}\gamma_\mu b)$ that induces DM scattering off detector nuclei only through a b-quark loop; the $m_V \gtrsim 300$ GeV range is ruled out.

(ii) Using a full collider simulation away from the contact-operator limit, we find that *existing* LHC sbottom searches at $\sqrt{s} = 8$ TeV strongly disfavor the axial-vector interaction $(\bar{\chi}\gamma^\mu\gamma_5\chi)(\bar{b}\gamma_\mu\gamma_5 b)$ for most combinations of perturbative couplings. While these searches have been used to constrain t-channel mediators that carry SM color charge (e.g. sbottoms) [15], this is the first work to highlight their sensitivity to uncolored s-channel mediators produced only through the interaction that also yields dark-matter annihilation. We also find these searches to be complementary to proposed mono-b + missing-energy searches [19], and we present 13 TeV projections for both.

(iii) The favored region for the pseudoscalar interaction $(\bar{\chi}\gamma^5\chi)(\bar{b}\gamma_5 b)$ is largely safe from both LHC and direct-detection bounds. Collider searches at 13 TeV are not sensitive to couplings that explain the Fermi excess.

In light of the strong constraints on the vector and axial-vector scenarios, we also considered two simple, renormalizable models that give rise to pseudoscalar-mediated $\chi\bar{\chi} \to b\bar{b}$ annihilation. One realization involves a two-Higgs doublet model in which one couples only to down-type quarks and mixes predominantly with a scalar that couples to DM. The other involves a DM coupled pseudoscalar and multiple flavors of vectorlike quarks. Integrating out the vectorlike states yields an effective

interaction between b quarks and DM and the pseudoscalar that parametrically depends on the ratio of Higgs VEV and vectorlike mass. Both models generically feature a suppressed pseudoscalar-b quark coupling.

ACKNOWLEDGMENTS

[1] J. Beringer *et al.* (Particle Data Group), Phys. Rev. D **86**, 010001 (2012).

[2] D. Hooper and L. Goodenough, Phys. Lett. B **697**, 412 (2011).

[3] A. Boyarsky, D. Malyshev, and O. Ruchayskiy, Phys. Lett. B **705**, 165 (2011).

[4] D. Hooper and T. Linden, Phys. Rev. D **84**, 123005 (2011).

[5] K. N. Abazajian and M. Kaplinghat, Phys. Rev. D **86**, 083511 (2012).

[6] D. Hooper, C. Kelso, and F. S. Queiroz, Astropart. Phys. **46**, 55 (2013).

[7] C. Gordon and O. Macias, Phys. Rev. D **88**, 083521 (2013).

[8] K. N. Abazajian, N. Canac, S. Horiuchi, and M. Kaplinghat, Phys. Rev. D **90**, 023526 (2014).

[9] T. Daylan, D. P. Finkbeiner, D. Hooper, T. Linden, S. K. N. Portillo *et al.*, arXiv:1402.6703.

[10] W.-C. Huang, A. Urbano, and W. Xue, arXiv:1307.6862.

[11] W.-C. Huang, A. Urbano, and W. Xue, J. Cosmol. Astropart. Phys. 04 (2014) 020.

[12] L. Goodenough and D. Hooper, arXiv:0910.2998.

[13] J. F. Navarro, C. S. Frenk, and S. D. White, Astrophys. J. **490**, 493 (1997).

[14] A. Alves, S. Profumo, F. S. Queiroz, and W. Shepherd, arXiv:1403.5027.

[15] A. Berlin, D. Hooper, and S. D. McDermott, Phys. Rev. D **89**, 115022 (2014).

[16] A. DiFranzo, K. I. Nagao, A. Rajaraman, and T. M. P. Tait, J. High Energy Phys. 11 (2013) 014.

[17] P. Agrawal, B. Batell, D. Hooper, and T. Lin, arXiv:1404.1373.

[18] C. Boehm, M. J. Dolan, C. McCabe, M. Spannowsky, and C. J. Wallace, J. Cosmol. Astropart. Phys. 05 (2014) 009.

[19] T. Lin, E. W. Kolb, and L.-T. Wang, Phys. Rev. D **88**, 063510 (2013).

[20] D. Akerib *et al.* (LUX Collaboration), Phys. Rev. Lett. **112**, 091303 (2014).

[21] D. B. Kaplan and A. Manohar, Nucl. Phys. **B310**, 527 (1988).

[22] J. Kopp, V. Niro, T. Schwetz, and J. Zupan, Phys. Rev. D **80**, 083502 (2009).

[23] R. H. Helm, Phys. Rev. **104**, 1466 (1956).

[24] P. Agrawal, S. Blanchet, Z. Chacko, and C. Kilic, Phys. Rev. D **86**, 055002 (2012).

[25] B. A. Dobrescu and F. Yu, Phys. Rev. D **88**, 035021 (2013).

[26] S. Chatrchyan *et al.* (CMS Collaboration), Phys. Lett. B **722**, 207 (2013).

[27] J. Alwall, M. Herquet, F. Maltoni, O. Mattelaer, and T. Stelzer, J. High Energy Phys. 06 (2011) 128.

[28] F. J. Petriello, S. Quackenbush, and K. M. Zurek, Phys. Rev. D **77**, 115020 (2008).

[29] Y. Gershtein, F. Petriello, S. Quackenbush, and K. M. Zurek, Phys. Rev. D **78**, 095002 (2008).

[30] Q.-H. Cao, C.-R. Chen, C. S. Li, and H. Zhang, J. High Energy Phys. 08 (2011) 018.

[31] M. Beltran, D. Hooper, E. W. Kolb, Z. A. Krusberg, and T. M. Tait, J. High Energy Phys. 09 (2010) 037.

[32] J. Goodman, M. Ibe, A. Rajaraman, W. Shepherd, T. M. Tait, and H.-B. Yu, Phys. Lett. B **695**, 185 (2011).

[33] Y. Bai, P. J. Fox, and R. Harnik, J. High Energy Phys. 12 (2010) 048.

[34] J. Goodman, M. Ibe, A. Rajaraman, W. Shepherd, T. M. Tait, and H.-B. Yu, Phys. Rev. D **82**, 116010 (2010).

[35] P. J. Fox, R. Harnik, J. Kopp, and Y. Tsai, Phys. Rev. D **84**, 014028 (2011).

[36] J.-F. Fortin and T. M. Tait, Phys. Rev. D **85**, 063506 (2012).

[37] M. T. Frandsen, F. Kahlhoefer, S. Sarkar, and K. Schmidt-Hoberg, J. High Energy Phys. 09 (2011) 128.

[38] A. Rajaraman, W. Shepherd, T. M. Tait, and A. M. Wijangco, Phys. Rev. D **84**, 095013 (2011).

[39] P. J. Fox, R. Harnik, J. Kopp, and Y. Tsai, Phys. Rev. D **85**, 056011 (2012).

[40] J. Goodman and W. Shepherd, arXiv:1111.2359.

[41] I. M. Shoemaker and L. Vecchi, Phys. Rev. D **86**, 015023 (2012).

[42] H. An, X. Ji, and L.-T. Wang, J. High Energy Phys. 07 (2012) 182.

[43] P. J. Fox, R. Harnik, R. Primulando, and C.-T. Yu, Phys. Rev. D **86**, 015010 (2012).

[44] M. T. Frandsen, F. Kahlhoefer, A. Preston, S. Sarkar, and K. Schmidt-Hoberg, J. High Energy Phys. 07 (2012) 123.

[45] Y. Bai and T. M. Tait, Phys. Lett. B **723**, 384 (2013).

[46] R. Cotta, J. Hewett, M. Le, and T. Rizzo, Phys. Rev. D **88**, 116009 (2013).

[47] L. M. Carpenter, A. Nelson, C. Shimmin, T. M. Tait, and D. Whiteson, Phys. Rev. D **87**, 074005 (2013).

[48] H. Dreiner, D. Schmeier, and J. Tattersall, Europhys. Lett. **102**, 51001 (2013).

[49] G. Busoni, A. De Simone, E. Morgante, and A. Riotto, Phys. Lett. B **728**, 412 (2014).

[50] Z.-H. Yu, Q.-S. Yan, and P.-F. Yin, Phys. Rev. D **88**, 075015 (2013).

[51] S. Profumo, W. Shepherd, and T. Tait, Phys. Rev. D **88**, 056018 (2013).

[52] H. An, L.-T. Wang, and H. Zhang, Phys. Rev. D **89**, 115014 (2014).

[53] O. Buchmueller, M. J. Dolan, and C. McCabe, J. High Energy Phys. 01 (2014) 025.

[54] J. Alwall, S. de Visscher, and F. Maltoni, J. High Energy Phys. 02 (2009) 017.

[55] J. M. Campbell and R. K. Ellis, Phys. Rev. D **65**, 113007 (2002).

[56] J. M. Campbell and R. K. Ellis, arXiv:1204.1513.

[57] T. Sjostrand, S. Mrenna, and P. Z. Skands, J. High Energy Phys. 05 (2006) 026.

[58] J. Conway, A Pretty Good Simulation (2009), http://physics.ucdavis.edu/~conway/research/software/pgs/pgs4-general.htm.

[59] R. Essig, E. Izaguirre, J. Kaplan, and J. G. Wacker, J. High Energy Phys. 01 (2012) 074.

[60] M. Cacciari, G. P. Salam, and G. Soyez, J. High Energy Phys. 04 (2008) 063.

[61] G. Aad et al. (ATLAS Collaboration), J. High Energy Phys. 10 (2013) 189.

[62] CMS Collaboration, Report No. CMS-PAS-SUS-13-018, CERN, Geneva (2014).

[63] J. Alwall, M.-P. Le, M. Lisanti, and J. G. Wacker, Phys. Lett. B **666**, 34 (2008).

[64] S. L. Glashow and S. Weinberg, Phys. Rev. D **15**, 1958 (1977).

[65] B. Batell, D. McKeen, and M. Pospelov, J. High Energy Phys. 10 (2012) 104.

[66] S. Chatrchyan et al. (CMS Collaboration), Phys. Lett. B **729**, 149 (2014).

[67] S. Chatrchyan et al. (CMS Collaboration), Technical Report No. ATLAS-CONF-2013-018, CERN, Geneva (2013).

[68] S. Chatrchyan et al. (CMS Collaboration), Technical Report No. CMS-PAS-TOP-12-003, CERN, Geneva (2013).

[69] S. Chatrchyan et al. (CMS Collaboration), Eur. Phys. J. C **73**, 2677 (2013).